

Effect of thermal fluctuations in topological p -wave superconductors

Bela Bauer,¹ Roman M. Lutchyn,¹ Matthew B. Hastings,^{1,2} and Matthias Troyer³

¹*Station Q, Microsoft Research, Santa Barbara, CA 93106-6105, USA*

²*Duke University, Department of Physics, Durham, NC 27708, USA*

³*Theoretische Physik, ETH Zurich, 8093 Zurich, Switzerland*

We study the effect of thermal fluctuations on the topological stability of chiral p -wave superconductors. We consider two models of superconductors: spinless and spinful with a focus on topological properties and Majorana zero-energy modes. We show that proliferation of vortex-antivortex pairs above the Kosterlitz-Thouless temperature T_{KT} drives the transition from a thermal Quantum Hall insulator to a thermal metal/insulator, and dramatically modifies the ground-state degeneracy splitting. Therefore, in order to utilize 2D chiral p -wave superconductors for topological quantum computing, the temperature should be much smaller than T_{KT} . Within the spinful chiral p -wave model, we also investigate the interplay between half-quantum vortices carrying Majorana zero-energy modes and full-quantum vortices having trivial topological charge, and discuss topological properties of half-quantum vortices in the background of proliferating full-quantum vortices.

PACS numbers: 03.65.Vf, 72.15.Rn, 74.40.+k

Topological phases of matter have been subject of intense physics research in the last decade [1]. In addition to interest from the fundamental physics point of view, these states of matter can also be used for topological quantum computation [2], which is predicted to have an exceptional fault-tolerance by virtue of encoding and manipulating information in non-local degrees of freedom of topologically ordered systems [3]. Candidate physical systems include Fractional Quantum Hall states [4], topological superconductors and superfluids [5, 6] and certain spin systems [3]. The common underlying features of all these systems is a ground-state degeneracy as well as the presence of certain quasiparticle excitations (non-Abelian anyons) whose manipulation allows one to process quantum information. In all these candidate physical systems the low-energy topological degrees of freedom coexist with some other (non-topological) degrees. It is important to understand their interplay since these non-topological degrees of freedom often determine the stability of the topological phase.

In this Letter we focus on 2D topological p -wave superconductors and study their robustness against thermal fluctuations. Specifically, we investigate topological degeneracy in these superconducting systems in the presence of thermally-generated topological defects (vortices). Without vortices, the stability condition for the topological superconducting phase is set by the quasiparticle energy gap Δ , *i.e.*, $T \ll T_c \sim \Delta$ [7]. We show here that vortex-antivortex proliferation provides a more stringent temperature requirement since T_{KT} can be much lower than the temperature scale defined by the quasiparticle gap.

We model thermal fluctuations with a classical XY model. As the temperature is increased above the Kosterlitz-Thouless (KT) transition point but still well below the scale of local quasiparticle gap ($T_{KT} < T \ll T_c$), vortices start to proliferate and eventually destroy

the topological phase by driving the system into a thermal metal or non-topological insulator phase. The degeneracy splitting in low temperature ($T < T_{KT}$) and high-temperature ($T > T_{KT}$) phases is different, changing from exponentially to power-law scaling with the system size.

A spinful model allows for two types of defects – half-quantum (HQV) and full-quantum (FQV) vortices. Only the former carry robust Majorana zero-energy modes. Thus, one can consider the interesting situation where the superconducting phase is disordered due to the presence of FQVs and study the degeneracy splitting due to the presence of HQVs embedded in the system at distance $R \gg \xi$ from each other. Naively, one might expect that the splitting would not be affected by the proliferation of FQVs since the splitting energy is governed by the local quasiparticle gap which is only weakly affected by thermal fluctuations. However, we show that the situation is much more intricate and requires a much deeper understanding of the interplay between topological and non-topological degrees of freedom.

It is well-known that in superconductors in symmetry class D [8], disorder can drive a transition from the thermal Quantum Hall (TQH) phase to either a thermal metal (TM) phase or a topologically trivial thermal insulator (TTI) [5, 9–13]. These phases have been primarily studied in the context of network models [11–13] and very recently in certain microscopic models [14, 15]. We find that we can realize all these phases in our microscopic model, where the disorder is generated by thermal fluctuations. The TTI is an insulator in the sense of Anderson localization albeit having a non-zero density of states at $E = 0$. We demonstrate that this phase does not realize the aforementioned scenario where the splitting is governed by the local quasiparticle gap even if the phase is disordered. Instead, the presence of modes at zero energy changes the splitting from exponential to

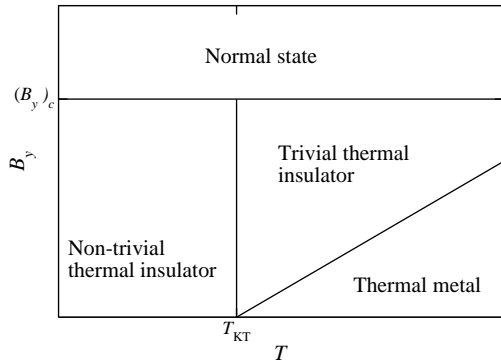


FIG. 1. Schematic phase diagram of a spinful p -wave superconductor as a function of temperature and in-plane magnetic field. The phase diagram of the spinless case is recovered for $B_y = 0$. Above $(B_y)_c$, the superconducting order parameter vanishes in a self-consistent calculation.

power-law. We assume throughout the paper that the system size is smaller than the localization length L_c .

Models and methods. We set up our numerical problem in two steps. In the first step, we model thermal fluctuations of the superconducting phase using a classical XY Hamiltonian. We then make an adiabatic approximation by assuming that the vortex dynamics is slow compared to the quasiparticle one which appears to be quite reasonable since Abrikosov vortices are macroscopic and have much higher mass. Under these conditions, quasiparticles are moving in a static background of different vortex configurations. As a second step, we diagonalize the Bogoliubov-de-Gennes Hamiltonian for each disorder realization and compute the quasiparticle energy spectrum as well as other physical quantities such as the density of states (DoS) and the inverse participation ratio (IPR).

We consider a model for a $p + ip$ superconductor on a torus of $L \times L$ sites, described by the Hamiltonian

$$H = \sum_{\langle i,j \rangle, \sigma, \sigma'} \left(t^{\sigma\sigma'} c_{i\sigma}^\dagger c_{j\sigma'} + \Delta_{ij}^{\sigma\sigma'} c_{i\sigma}^\dagger c_{j\sigma'}^\dagger + h.c. \right) - \mu \sum_{i\sigma} c_{i\sigma}^\dagger c_{i\sigma} \quad (1)$$

We first study spinless p -wave superconductor model by assuming that $t^{\sigma\sigma'} = -t\delta_{\sigma,\sigma'}$ and choosing an order parameter $\Delta_{ij}^{\sigma\sigma'}$ to be decoupled in the spin sectors. This corresponds to a \hat{d} -vector characterizing spin-triplet pairing to be aligned along \hat{x} -axis [16], $\Delta_{ij}^{\sigma\sigma'} = \delta_{\sigma\sigma'} \Delta_0 \chi_{ij} \theta_{ij}$; μ is chemical potential. Unless spin-mixing perturbations are added, we can equivalently study a spin-polarized system. χ_{ij} is a chirality factor that implements $p + ip$ pairing: $\chi_{ij} = \pm 1$ for $j = i \pm \hat{x}$, and $\pm i$ for $j = i \pm \hat{y}$. θ_{ij} is a phase variable to be discussed below, and Δ_0 is chosen to be a constant [17]. We solve the corresponding BdG equation numerically to obtain eigenvalues E_n and

eigenstates $(u_n, v_n)^T$.

Vortices in the order parameter of a spinless p -wave superconductor bind Majorana zero-energy modes, i.e. modes with $E = 0$ for which $u = v^*$ [5]. These localized quasiparticles are described by a self-conjugate operator $\gamma = \gamma^\dagger$. The ground state degeneracy as well as the presence of Majorana quasiparticles bound to vortices ultimately leads to non-Abelian braiding statistics in these many-particle systems [16, 18–20]. Depending on parameters, vortices may carry a large number of localized states below the bulk gap. To reduce the required computational effort, we typically use $\Delta \sim \mu$ where no midgap states except the zero-energy state are present. The effect of such midgap states has been discussed in Ref. [21].

The situation becomes more subtle when many vortices are present and localized zero-energy modes hybridize leading to a ground-state degeneracy splitting [22–25]. At large vortex separation $R \gg \xi$, Majorana modes acquire an exponentially small energy splitting and the ground-state degeneracy at small vortex density is preserved only up to exponentially small corrections. Specifically, the splitting energy δE in p -wave superconductors reads [22, 26]

$$\delta E_{12} \sim (kR_{12})^{-1/2} Y(kR_{12}) \exp(-R_{12}/\xi) \quad (2)$$

where $Y(kR)$ is an oscillatory function, $k = \sqrt{k_F^2 - \Delta_0^2/v_F^2}$ with k_F being Fermi momentum and $R_{12} \gg \max(k^{-1}, \xi)$ (for the full expression, see the supplementary material [17]). Thus, the effective low-energy model for multi-vortex configuration reads $H = i \sum_{ij} \delta E_{ij} \gamma_i \gamma_j$, where γ_j is a self-conjugate (Majorana) operator representing a zero-energy state in j -th vortex. Given that in realistic systems $kR_{ij} \gg 1$, δE_{ij} is a rapidly oscillating function.

We now study how this exponential ground-state degeneracy is modified by vortex-antivortex proliferation above the KT transition. We consider a situation where thermal fluctuations affect only the phase of the order parameter while the magnitude remains approximately constant [17]. The fluctuations of the phase can be modeled by a classical XY Hamiltonian for the bond phases θ_{ij} ,

$$H = -J \sum \cos(\arg \theta_{ij} - \arg \theta_{jk}), \quad (3)$$

where J represents superfluid stiffness. A key property of this model is that below the KT temperature ($T_{KT} = 0.89J$ in the infinite system [27, 28]), vortices/antivortices are bound in pairs by a logarithmic attraction. Above the transition, they unbind and proliferate. The Monte Carlo sampling is performed using a standard cluster update method [27, 29]. To study the effect of thermal fluctuations on the topological degeneracy, we introduce a fixed vortex/antivortex pair in the system by adding a

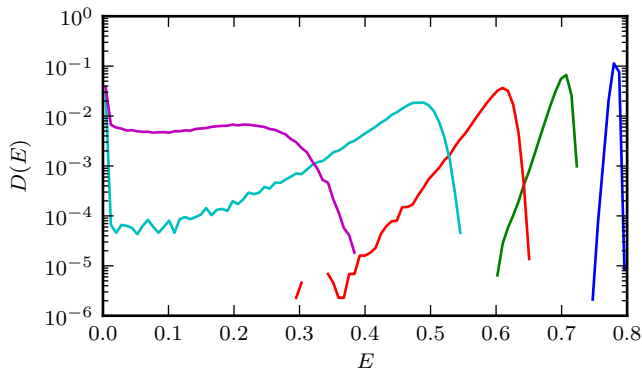


FIG. 2. Density of states $D(E)$ in the low-temperature phase ($T = 0.1, 0.3, 0.5, 0.7, 0.9$, from right to left) for $L = 64$. Clearly, the density of states is strongly suppressed for sufficiently low temperatures and only shows a peak close to zero energy corresponding to a slightly renormalized value of the energy of the $T = 0$ case, and an increase as the transition is approached. Simulations were performed for $\Delta_0 = t/2$ and $\mu = -t$.

non-fluctuation phase factor to Δ_{ij} (see the supplementary material [17]) and study the energy splitting in the presence of the background defects.

Diagonalizing the BdG equation for each configuration of θ_{ij} , we compute the DoS

$$D(E) = \frac{1}{N} \left\langle \sum_n \delta(E - E_n) \right\rangle_T, \quad (4)$$

where $\langle \cdot \rangle_T$ indicates the Monte Carlo average at temperature T , and N denotes the number of states. We generally average over 10,000 configurations; in some cases, we average over up to 500,000 configurations. The error bars shown have been obtained with a standard Jackknife analysis. As shown in Fig. 2, the density of states at zero temperature shows a sharp peak at the energy splitting set by the system size for the fixed vortices, and a continuum of states above the bulk gap Δ_0 . At low temperatures $T \ll T_{KT}$, both features are broadened but the energy splitting of the Majorana modes remains exponential and that the density of states is suppressed between this scale and the bulk gap.

To further elucidate the fate of the ground-state degeneracy, we study the energy splitting between fixed vortices as a function of temperature by fitting it to (cf. Eqn. (2))

$$\delta E = \frac{c_1}{\sqrt{R}} \exp\left(-\frac{x}{\xi}\right) (1 + c_2 \cos(c_3 x + c_4)), \quad (5)$$

where ξ , c_1 , c_2 , c_3 and c_4 are fit parameters. Good agreement is obtained for low temperatures, as shown in the inset of Fig. 3. Our results for the correlation length are shown in the main panel of that figure. The correlation length depends only weakly on temperature as long as

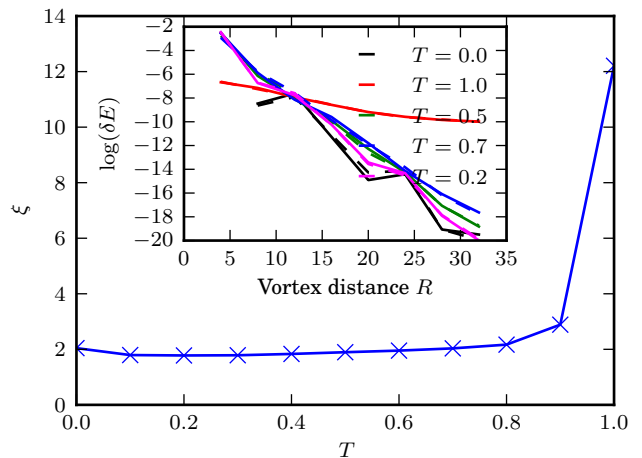


FIG. 3. Scaling of the energy splitting with vortex distance d in a system of size $L = 64$. The main panel shows the dependence of the coherence length ξ on the temperature that governs the phase fluctuations. A KT transition takes place at $T \sim 0.9$. The inset shows the dependence of the splitting ϵ of Majorana vortices on the distance with a fit to Eqn. (5). Simulations were performed for $\Delta_0 = t/2$ and $\mu = -t$.

the system is well below the KT transition. At the transition, a sharp jump in the correlation length is observed which indicates a fundamental change in the scaling behavior.

The sharp change of the localization function is related to the delocalization transition (*i.e.* appearance of a disorder-driven thermal metal phase) characteristic to class D superconductors [9, 12, 13, 15]. The TM is characterized by delocalized states at $E = 0$ and a logarithmic divergence of the density of states for low energies [15, 30]. Furthermore, oscillatory behavior of the density of states in the zero-dimensional limit is consistent with the random matrix theory predictions for class D [8]. In Fig. 4, the density of states for a spinless p -wave superconductor well above the KT transition is shown along with a fit to the random matrix theory result [8]

$$D(E) \sim \gamma + \frac{\sin(2\pi\gamma EL^2)}{2\pi EL^2} \quad (6)$$

for symmetry class D . Using a single-parameter fit, we obtain an excellent agreement with our theoretical expectations for the thermal metal phase: i) At the lowest energy scale, the density of states follows the prediction of random matrix theory. ii) For higher energy scales (but still well below the superconducting gap Δ), a characteristic logarithmic divergence is observed. This clearly establishes that our model realizes a thermal metal phase above the KT transition, as shown along the $B_y = 0$ line in Fig. 1.

The coefficient γ above is related to the effective bandwidth in the Majorana fermion hopping problem defined above and should, therefore, be related to δE (2). In-

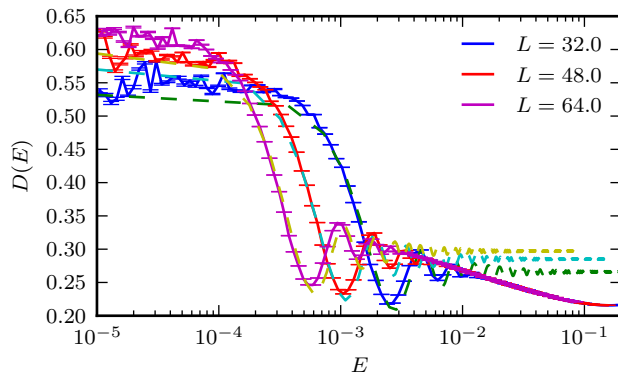


FIG. 4. Density of states $D(E)$ in the high-temperature phase ($T = 1.5$, $\Delta_0 = t/2$, $\mu = -t$). Fits are to Eqn. (6). The data has been rescaled such that $D(0.03) = 1$.

deed, we numerically confirm that $\gamma \sim \Delta_0 \exp(-\Delta_0/C)$ for some constant C . The energy scale is largely independent of temperature as long as the temperature is sufficiently far away from the KT transition.

We now consider perturbations breaking $SU(2)$ symmetry. HQVs correspond to a phase twist only in one spin sector and so still carry Majorana zero-energy modes. However, FQVs do not carry robust zero-energy modes. When adding a perturbation corresponding to a Zeeman splitting generated by an in-plane magnetic field $B_y \sum_i (ic_{i\uparrow}^\dagger c_{i\downarrow} - ic_{i\downarrow}^\dagger c_{i\uparrow})$, the lowest excitation energy supported by an FQV moves to non-zero $E_0 = B_y$.

Indeed for each pair of wavefunctions of the spinless model at energies $\pm E$, there are four wavefunctions at energies $\pm E \pm B_y$ when the spin degeneracy is lifted with this special choice of field direction. Thus, if the system has a band of delocalized states near $E = 0$, the system will remain in a thermal metal phase for B_y smaller than the width of this band and will transition to an insulating phase once B_y is larger than the width of this band. To determine this width, in Fig. 5 we show the DoS and the localization properties of the states, which we characterize by the inverse participation ratio (IPR) $I(E)$ defined to be the average of the *fourth* moment of a wavefunction of energy E . For extended states, the IPR is expected to scale with a power law, $I(E) \sim L^{2-\nu}$, where ν is a non-universal correction to the exponent [31] (there may also be logarithmic corrections) while the IPR is expected to approach a constant for localized states, $\lim_{L \rightarrow \infty} I(E) > 0$. An analysis of the scaling of the IPR with L is shown in the bottom panel Fig. 5. While Fig. 5 supports having delocalized states only at energy $E = B_y$, analysis at higher temperatures shows a band of delocalized states with non-zero width, supporting the hypothesis of Fig. 1 of a thermal metal up to non-zero B_y . For details, refer to the supplemental material [17]. We have checked the robustness of our result against other perturbations, such as an additional

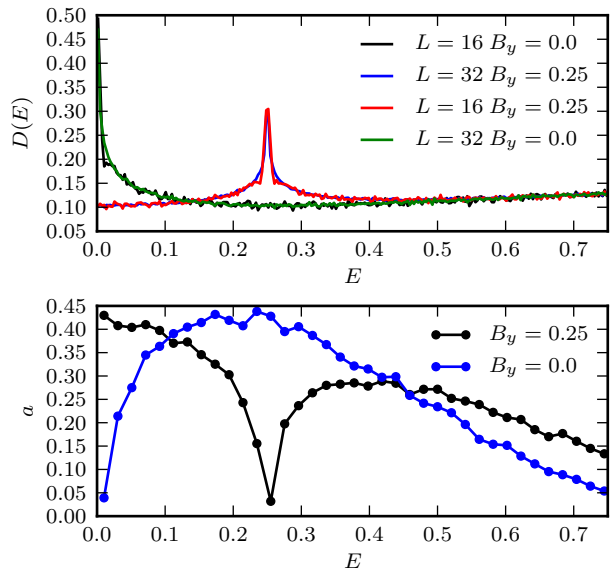


FIG. 5. Top panel: Density of states for spinful fermions for two different system sizes. With magnetic field, the density of states has a constant value at $E = 0$, whereas without magnetic field it diverges due to the thermal metal. In the case with magnetic field, a peak appears at $E = B_y$. Finite-size scaling of the IPR to distinguish energy ranges with localized and delocalized states. The figure shows the constant term obtained from a fit to $I \sim a + L^b$. Values of $a \rightarrow 0$ and $a \neq 0$ indicate extended and localized states, respectively.

magnetic field $B_x \sum_i (c_{i\uparrow}^\dagger c_{i\downarrow} + c_{i\downarrow}^\dagger c_{i\uparrow})$. At this point, it remains an open question whether these states are truly extended and how this can be connected to theoretical work.

One can now ask about the fate of the Majorana zero-energy modes carried by HQVs in the TTI phase. To investigate this, we study the density of states with two fixed HQVs in the background of thermally fluctuating FQVs. As shown in the inset of Fig. 6, two HQVs give rise to an additional contribution to the density of states at low energies. By studying the energy splitting as a function of the temperature, we find that the correlation length ξ that governs the splitting energy in Eq. (2) changes qualitatively at the KT transition, see Fig. 6. Our small system sizes do not let us determine whether the splitting is still exponential or becomes power law in this regime. In any case, we find that the splitting energy for HQVs in chiral p -wave superconductors changes dramatically above the KT transition. Thus, thermal disordering of the superconducting phase by HQVs leads to drastic change of the topological properties of chiral p -wave superconductors which is a main result of this paper.

We acknowledge useful discussions with Matthew Fisher, Andreas Ludwig and Simon Trebst. We would like to thank the Aspen Center for Physics where this

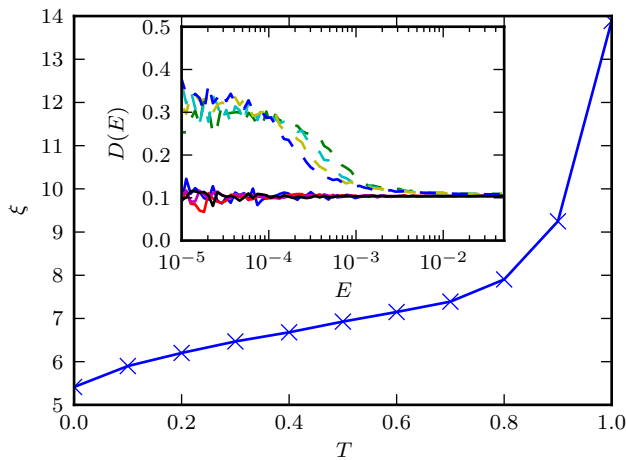


FIG. 6. Main panel: correlation length ξ for HQVs extracted from an analogous fit to Eqn. (5). The correlation length displays a clear jump at the KT transition. Inset: DoS for a system in the thermal insulator phase ($B_y = 0.25$, $\Delta = t$, $\mu = -2t$, $L = 40, 48, 56, 64$) with (dashed lines) and without (solid lines) fixed HQVs. Simulations for the inset for run with $T = 1.5$.

work was initiated. Simulations were performed using the ALPS libraries [32].

[1] F. Wilczek, *Nature Physics* **5**, 614 (2009); C. Nayak, *Nature* **464**, 693 (2010); M. Franz, *Physics* **3**, 24 (2010); A. Stern, *ibid.* **464**, 187 (2010).
 [2] S. D. Sarma, M. Freedman, and C. Nayak, *Physics Today* **59**, 32 (2006).
 [3] A. Y. Kitaev, *Ann. Phys. (N.Y.)* **303**, 2 (2003), [quant-ph/9707021](#); M. H. Freedman, *Proc. Natl. Acad. Sci. USA* **95**, 98 (1998); C. Nayak, S. H. Simon, A. Stern, M. Freedman, and S. D. Sarma, *Rev. Mod. Phys.* **80**, 1083 (2008).
 [4] G. Moore and N. Read, *Nucl. Phys. B* **360**, 362 (1991).
 [5] N. Read and D. Green, *Phys. Rev. B* **61**, 10267 (2000).
 [6] L. Fu and C. L. Kane, *Phys. Rev. Lett.* **100**, 096407 (2008), [arXiv:0707.1692](#); J. D. Sau, R. M. Lutchyn, S. Tewari, and S. Das Sarma, *ibid.* **104**, 040502 (2010).
 [7] M. Cheng, R. M. Lutchyn, and S. Das Sarma, *ArXiv e-prints* (2011), [arXiv:1112.3662](#).
 [8] A. Altland and M. R. Zirnbauer, *Phys. Rev. B* **55**, 1142 (1997).
 [9] M. Bocquet, D. Serban, and M. Zirnbauer, *Nuclear Physics B* **578**, 628 (2000).
 [10] S. Vishveshwara, T. Senthil, and M. P. A. Fisher, *Phys. Rev. B* **61**, 6966 (2000).
 [11] I. A. Gruzberg, N. Read, and A. W. W. Ludwig, *Phys. Rev. B* **63**, 104422 (2001).
 [12] J. T. Chalker, N. Read, V. Kagalovsky, B. Horovitz, Y. Avishai, and A. W. W. Ludwig, *Phys. Rev. B* **65**, 012506 (2001).
 [13] A. Mildenberger, F. Evers, A. D. Mirlin, and J. T. Chalker, *Phys. Rev. B* **75**, 245321 (2007).

[14] M. V. Medvedyeva, J. Tworzydło, and C. W. J. Beenakker, *Phys. Rev. B* **81**, 214203 (2010).
 [15] C. R. Laumann, A. W. W. Ludwig, D. A. Huse, and S. Trebst, *Phys. Rev. B* **85**, 161301 (2012).
 [16] D. A. Ivanov, *Phys. Rev. Lett.* **86**, 268 (2001).
 [17] See supplemental material, page 6.
 [18] A. Stern, F. von Oppen, and E. Mariani, *Phys. Rev. B* **70**, 205338 (2004).
 [19] N. Read, *Phys. Rev. B* **79**, 045308 (2009).
 [20] P. Bonderson, V. Gurarie, and C. Nayak, *Phys. Rev. B* **83**, 075303 (2011).
 [21] M. Cheng, R. M. Lutchyn, and S. Das Sarma, *Phys. Rev. B* **85**, 165124 (2012).
 [22] M. Cheng, R. M. Lutchyn, V. Galitski, and S. Das Sarma, *Phys. Rev. Lett.* **103**, 107001 (2009).
 [23] M. Baraban, G. Zikos, N. Bonesteel, and S. H. Simon, *Phys. Rev. Lett.* **103**, 076801 (2009).
 [24] P. Bonderson, *Phys. Rev. Lett.* **103**, 110403 (2009).
 [25] V. Lahtinen, *New Journal of Physics* **13**, 075009 (2011).
 [26] M. Cheng, R. M. Lutchyn, V. Galitski, and S. Das Sarma, *Phys. Rev. B* **82**, 094504 (2010).
 [27] U. Wolff, *Nuclear Physics B* **322**, 759 (1989).
 [28] R. Gupta and C. F. Baillie, *Phys. Rev. B* **45**, 2883 (1992).
 [29] U. Wolff, *Phys. Rev. Lett.* **62**, 361 (1989).
 [30] T. Senthil and M. P. A. Fisher, *Phys. Rev. B* **61**, 9690 (2000).
 [31] F. Wegner, *Zeitschrift für Physik B Condensed Matter* **36**, 209 (1980); V. I. Fal'ko and K. B. Efetov, *EPL (Europhysics Letters)* **32**, 627 (1995); *Phys. Rev. B* **52**, 17413 (1995).
 [32] B. Bauer *et al.*, *Journal of Statistical Mechanics: Theory and Experiment* **2011**, P05001 (2011).

SUPPLEMENTARY MATERIAL: EFFECT OF THERMAL FLUCTUATIONS IN TOPOLOGICAL p -WAVE SUPERCONDUCTORS

In the supplementary material, technical details of how our model is set up will be discussed. In addition, we discuss details of our calculation of the inverse participation ratio and an alternative approach of defining the characteristic energy scale of HQVs in the trivial thermal insulator phase.

Homogeneous solution In the homogeneous case $\theta_{ij} = 1$, the dispersion of the Hamiltonian is

$$\epsilon(k) = -\mu - 2t(\cos(k_x) + \cos(k_y)) \quad (7)$$

$$E(k) = \sqrt{\epsilon(k)^2 + \Delta_0(\sin^2(k_x) + \sin^2(k_y))}. \quad (8)$$

The dispersion has gapless points for $\mu = -4t, 0, 4t$.

The full expression for the energy splitting of two vortices at distance $R \gg \max(k^{-1}, \xi)$ reads:

$$\delta E = \sqrt{\frac{8}{\pi}} \frac{\mathcal{N}_1^2}{m} \left(\frac{\lambda^2}{1 + \lambda^2} \right)^{1/4} \frac{Y(kR)}{\sqrt{kR}} \exp\left(-\frac{R}{\xi}\right) \quad (9)$$

$$Y(kR) = \cos(kR + \alpha) - \frac{2}{\lambda} \sin(kR + \alpha) + \frac{2(1 + \lambda^2)^{1/4}}{\lambda}, \quad (10)$$

with $\lambda = k\xi$, $2\alpha = \arctan \lambda$, $k = \sqrt{2m\mu - \Delta_0^2}/v_F^2$, the Fermi velocity v_F and superconducting coherence length ξ .

Fixed vortices and gauge transformation We implement a fixed vortex-antivortex pair by introducing an additional phase factor,

$$\theta_{ij} = \exp(i\phi_{ij}) = \exp(i\phi_{ij}^A) \exp(-i\phi_{ij}^B). \quad (11)$$

Here ϕ_{ij}^A (ϕ_{ij}^B) are the polar angles that the bond ij has with the vortex (antivortex) located at position A (B). When applying this to a torus mapped to a lattice with periodic boundary conditions, special care has to be taken that the order parameter is smooth around the boundary.

To obtain a simpler description on the torus, we perform a gauge transformation after which the vortices are implemented only by a π phase shift in both hopping terms across a particular line (branch cut) connecting the two vortices. To this end, we introduce a gauge field ϕ_i on the sites such that $\phi_{ij} = (\phi_i + \phi_j)/2$ and perform the gauge transformation $c_i \rightarrow c_i \exp(-i\phi_i)$. For a single vortex, the field ϕ_i would wind from 0 to π around the vortex, whereas ϕ_{ij} would wind from 0 to 2π ; therefore $\exp(i\phi_{ij})$ is smooth, while $\exp(-i\phi_i)$ has a jump from -1 to 1 at a branch cut. It follows that everywhere except along this branch cut, $\exp(-i\phi_i) \exp(-i\phi_j) \exp(-i\phi_{ij}) = 1$ and the phase is removed from the anomalous hopping; along this branch cut, a phase π remains and hopping

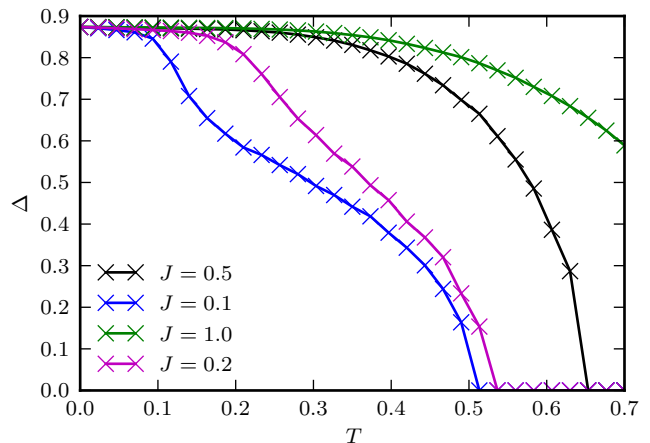


FIG. 7. Self-consistent calculation for Δ for lattice of size $L = 16$ and $U = 5$. The Kosterlitz-Thouless transition takes place at $T/J = 0.89$ and leads to the first drop in the gap Δ , which renormalizes it quantitatively while the system remains in a superconducting phase. For even higher temperatures, the gap vanishes and the superconductivity is destroyed.

terms with i and j on different sides of the branch cut pick up a minus sign. For the situation of two vortices, this can be generalized and one finds that the branch cut turns into a line connecting the two vortices. Applying the gauge transformation in the normal hopping, one finds that the same phase factor across the branch cut is introduced.

Self-consistency Owing to the mean-field approximation, the BdG equations have to be augmented with self-consistency conditions, which read

$$\Delta_{ij} = U \langle c_i c_j \rangle \quad (12)$$

$$= U \sum_{E_n > 0} u_n^*(i) v_n(j) \tanh\left(\frac{E_n}{2T}\right) \quad (13)$$

$$\Delta_0 = \langle |\Delta_{ij}| \rangle \text{ (spatial and MC average)}. \quad (14)$$

We have performed self-consistent calculations for a spinless p -wave superconductor without fixed vortices and obtained the order parameter $\Delta = \sqrt{\langle c_i c_j \rangle^2}$ as a function of temperature. Our results are shown in Fig. 7 for different values of J , which controls the relative temperature scales of the Kosterlitz-Thouless transition and the mean-field transition where superconductivity is destroyed. Our data show that for sufficiently small J , these two transitions are well-separated and there is an intermediate regime where the phase of the order parameter is disordered, but its magnitude remains finite at a value 20-30 % below the zero-temperature result. Since we are interested in qualitative results only, such a small qualitative change is irrelevant and we do not perform a self-consistent calculation but fix a value of Δ_0 independent of temperature.

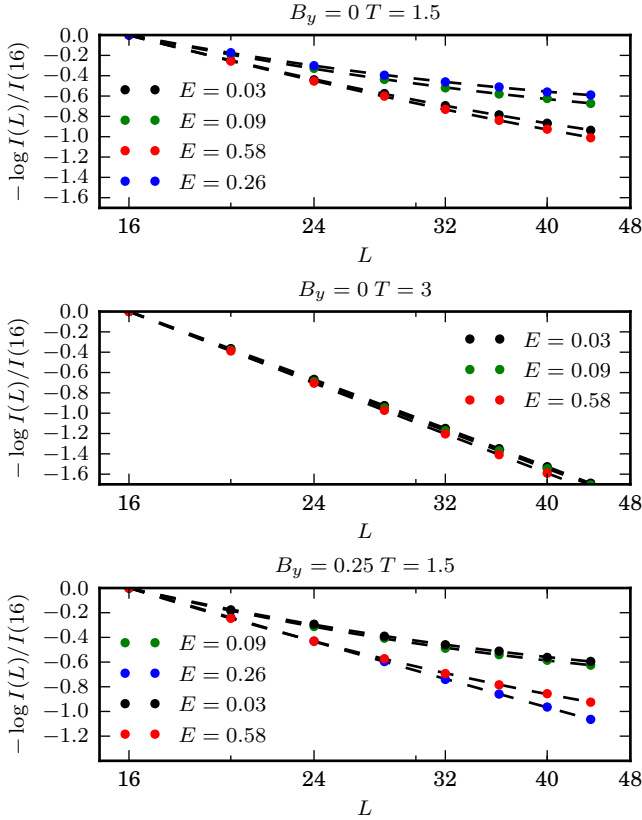


FIG. 8. Fit of the IPR to $I \sim a + L^b$ for several parameters sets. The top panel shows $\alpha = 0$, $T = 1.5$; the center panel shows $B_y = 0$, $T = 3$, and the bottom panel shows $B_y = 0.25$, $T = 1.5$. At $T = 1.5$, there is clearly only a very narrow band of delocalized states around $E \sim B_y$. For $T = 3$, however, the band is broadened such that states at almost all energies appear delocalized for the system sizes we can access.

IPR The inverse participation ratio can be calculated in our setup using

$$I(E) = \left\langle \sum_n \frac{\langle u_n \rangle^4 + \langle v_n \rangle^4}{(\langle u_n \rangle^2 + \langle v_n \rangle^2)^2} \delta(E - E_n) \right\rangle_T. \quad (15)$$

For finite systems, the IPR must be calculated by averaging over states in a finite range of energies centered around E . In the thermal metal phase, we expect $I(E)$ to scale with a power law at zero energy due to the presence of extended states. At non-zero energies, it is expected to approach a constant value for $L \rightarrow \infty$. In all cases, we expect it to behave with a power law for energies higher than the local gap Δ .

Figure 8 shows several fits for the IPR for two different values of the magnetic field, $B_y = 0$ and $B_y = 0.25$, and two different temperatures $T = 1.5$ and $T = 3$. The constant terms extract from such fits for $T = 1.5$ are shown in Fig. 5. The top panel ($B_y = 0$, $T = 1.5$) clearly shows the saturation of the IPR for energies $0 < E < \Delta$,

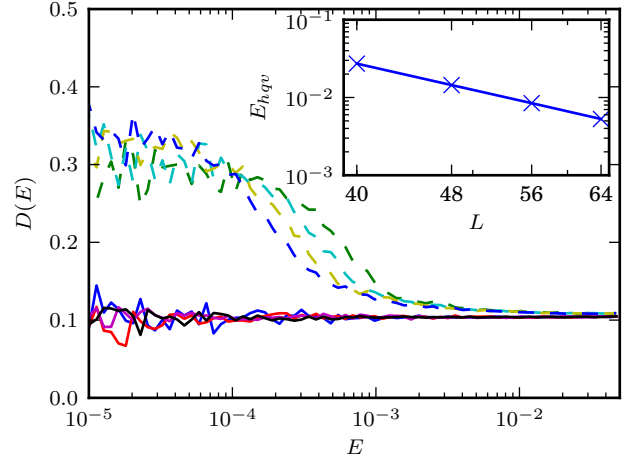


FIG. 9. Contribution of two fixed half-quantum vortices to the density of states in the high-temperature phase of a spinful superconductor with finite magnetic field. The main panel shows the density of states (solid lines: with HQVs, dashed lines: without HQVs). The scaling of the characteristic energy scale E_{hqv} , defined below Eqn. (16), is shown in the inset on a log-log scale.

whereas for very small energies, such as $E = 0.03$, no clear sign of saturation is observed for the accessible system sizes. The middle panel shows the same situation for a higher temperature, $T = 3$. In this case, the IPR appears to follow a power law also for intermediate energies such as $E = 0.09$. This is indicative of a delocalized band of finite width centered around $E = 0$, with the bandwidth growing as T is increased. Finally, the bottom panel shows the situation with finite magnetic field and temperature close to the KT transition, where no localization is observed around $E = B_y$.

HQVs As an alternative approach to quantify the energy scale below which half-quantum vortices contribute, we study the integrated difference between the density of states with, $D^h(E)$, and without, $D(E)$, half-quantum vortices:

$$\rho(E) = \int_0^E dE' (D^h(E') - D(E')) \quad (16)$$

and define E_{hqv} as the lowest energy such that $N\rho(E_{hqv}) = 1$, where $N = 2L^2$.

Fig. 9 shows the density of states with and without half-quantum vortices (cf. inset of Fig. 6). In the inset, the scaling of this quantity with system size is shown. A power-law scaling is clearly observed. This is consistent with the observation that the expectation value of the lowest energy $\langle E_0 \rangle_T$ behaves like a power-law both with and without HQVs. This shows that the topological degeneracy is destroyed by the presence of zero-energy states due to disorder, even though these states are localized.